column oxygen O(5) occupying the 3(*b*) position at ($\frac{1}{3}$, $\frac{2}{3}$, $\frac{1}{6}$). The conduction planes lie at $z = \frac{1}{6}$, $\frac{1}{2}$ and $\frac{5}{6}$ in the unit cell, although the conduction pathways can be described more exactly as undulating from 0·16 Å above the mean plane at a 6(*c*) site (an *up* site), *via* a symmetry centre at a 9(*d*) site, to 0·16 Å below the plane at a 6(*c*) site (a *down* site). We note that all sites are significantly less than fully occupied. The occupations refined within the $R3m$ space group are 20·5, 13·2, and 17·8% in the 6(*c*) (*up*), 9(*d*) and 6(*c*) (*down*) sites, respectively. As in the case of Ba^{2+} β''-alumina and Ca^{2+} β''-alumina, the average Sr^{2+}-ion distribution is better described in the noncentrosymmetric space group $R3m$, suggesting short-range correlation effects. The collection of the complete data set under the absence condition $-h+k+l \neq 3n$ implies that we do not have access to data capable of giving evidence of short-range symmetry lower than rhombohedral. That no significantly observed reflections appeared outside the $-h+k+l = 3n$ condition in the preliminary data set (out to $\theta = 10°$) implies that any divergence at short range from rhombohedral symmetry must be small.

Two general features can be noted in the Sr^{2+} distribution:

(i) The ratio of the refined 6(*c*) (*up*) to 6(*c*) (*down*) occupations (or *vice versa*) is ~1·5:1, compared to ~2·0:1 in Ca^{2+} β''-alumina and ~3·5:1 in Ba^{2+} β''-alumina. On the basis of earlier discussions for the Ca^{2+} and Ba^{2+} cases, the lower ratio would here suggest a shorter correlation length for the short-range ordering of the Sr^{2+} ions.

(ii) The majority of Sr^{2+} ions (61%) occupy the 9(*d*) mid-oxygen (*MO*) site, compared to 47% in Ca^{2+} β''-alumina and only 15% in Ba^{2+} β''-alumina.

In view of the equivalent electronic configurations of the three ion types studied (Ca^{2+}, Sr^{2+} and Ba^{2+}), it is tempting to seek some simple unifying picture to explain the qualitatively different average ionic distributions. A simple argument would be as follows: while Ba^{2+} ions are too large to occupy *MO* sites to any significant extent, both Ca^{2+} and Sr^{2+} ions fit comfortably into both *MO* and 6(*c*) end sites. Since the occupation of an *MO* site will tend to induce a transition from a local region of *up* dominance to an equivalent *down* region, the larger the *MO* occupation, the shorter will be the SRO correlation length, and the closer to 1·0 the 6(*c*) *up* to 6(*c*) *down* occupation ratio. This is indeed what we observe: a larger *MO* occupation for Sr^{2+} can be related to the lower *up*/*down* ratio. It must be stressed, however, that the observed average ionic distribution assumes translational symmetry for the unit-cell content. This is certainly not true for the X^{2+} ions. Arguments of the above type are therefore highly tenuous.

This research has been supported in part by the Swedish Natural Science Research Council, and in part by the United States Office of Naval Research under contract No. N00014-81-K-0526.

References

ALDÉN, M., THOMAS, J. O. & FARRINGTON, G. C. (1984). *Acta Cryst.* C**40**, 1763–1766.
BETTMAN, M. & PETERS, C. R. (1969). *J. Phys. Chem.* **73**, 1774–1780.
BROWN, G. M., SCHWINN, D. A., BATES, J. B. & BRUNDAGE, W. E. (1981). *Solid State Ionics*, **5**, 147–150.
DUNN, B. & FARRINGTON, G. C. (1980). *Mater. Res. Bull.* **15**, 1773–1774.
FARRINGTON, G. C. & DUNN, B. (1982). *Solid State Ionics*, **7**, 267–281.
International Tables for X-ray Crystallography (1974). Vol. IV. Birmingham: Kynoch Press. (Present distributor D. Reidel, Dordrecht.)
LUNDGREN, J.-O. (1982). *Crystallographic Computer Programs.* Report UUIC-B13-04-05. Inst. of Chemistry, Univ. of Uppsala.
SHANNON, R. D. (1976). *Acta Cryst.* **32**, 751–767.
THOMAS, J. O., ALDÉN, M., MCINTYRE, G. J. & FARRINGTON, G. C. (1984). *Acta Cryst.* B**40**, 208–213.

Acta Cryst. (1985). C**41**, 1703–1707

Multicomponent Polyanions. 38. Structure of $K_5NaMo_6V_2O_{26}.4H_2O$, a Compound Containing a New Configuration of the Hexamolybdodivanadate Anion

BY ANN-MARIE NENNER

Department of Inorganic Chemistry, University of Umeå, S-901 87 Umeå, Sweden

(*Received* 15 *April* 1985; *accepted* 15 *August* 1985)

Abstract. Pentapotassium sodium hexamolybdodivanadate tetrahydrate, $M_r = 1384{\cdot}1$, monoclinic, $C2/m$, $a = 14{\cdot}765$ (2), $b = 12{\cdot}859$ (1), $c = 9{\cdot}062$ (1) Å, $\beta = 127{\cdot}97$ (1)°, $V = 1356{\cdot}4$ (3) Å^3, $Z = 2$, $D_m = 3{\cdot}35$ (3), $D_x = 3{\cdot}39$ Mg m^{-3}, Mo $K\bar{\alpha}$, $\lambda = 0{\cdot}71069$ Å, $\mu = 4{\cdot}156$ mm^{-1}, $F(000) = 1304$, $T = 298$ K, $R = 0{\cdot}043$

0108-2701/85/121703-05$01.50

for 3970 unique observed reflexions. The structure contains $Mo_6V_2O_{26}^{6-}$ anions joined together in a three-dimensional framework by electrostatic O—Na—O and O—K—O linkages as well as by hydrogen bonds. The anion, which is isostructural with the octamolybdate anion (β-$Mo_8O_{26}^{4-}$) [Lindqvist (1950). *Ark. Kemi*, **2**, 349–355], consists of six MoO_6 and two VO_6 octahedra connected by shared edges. The MoO_6 octahedra have two and the VO_6 octahedra one terminal O. The short Mo—Mo, Mo—V and V—V distances are 3·24–3·34, 3·12–3·44 and 3·49 Å, respectively. The distances within the anion can be separated into three groups: (i) short *M*—O bonds [Mo 1·71–1·74 Å, V 1·62(terminal O)–1·72 Å], (ii) intermediate *M*—O bonds (Mo 1·91–1·96 Å, V 1·92 Å) and (iii) long *M*—O bonds (Mo 2·21–2·44 Å, V 2·13–2·34 Å). Every anion is surrounded by 18 cations (two Na^+ and 16 K^+). The Na^+ cation is surrounded by six anion O (Na—O 2·40–2·57 Å). One of the two crystallographically independent K^+ cations is surrounded by eight anion O (K—O 2·90–3·19 Å) and the other by seven anion O and two water O (K—O 2·76–3·15 Å).

Introduction. This study forms part of a project aimed at explaining the aqueous equilibria and structures of three-component complexes in the system H^+–MoO_4^{2-}–$H_2VO_4^-$. The similarity in size and coordination towards O by Mo^{VI} and V^V gives every reason to expect numerous compositional and structural combinations. A great number of molybdovanadates, with Mo/V ratios between 6/1 and 1/8, have also been reported (Mellor, 1964).

Our investigation began with potentiometric titrations but, due to the variety of complexes formed, interpretation of the data proved to be very difficult (Pettersson, 1984). To support the results with information about possible compositions and configurations, crystallization experiments followed by X-ray investigations were started. Four structures have been previously reported, all containing different types of heteropolyanions: $Na_6Mo_6V_2O_{26}.16H_2O$ (Björnberg, 1979*b*), $K_8Mo_4V_8O_{36}.12H_2O$ (Björnberg, 1979*a*), $K_7Mo_8V_5O_{40}.{\sim}8H_2O$ (Björnberg, 1980) and the mixed-valence species $K_6(V^{IV}V^VMo_{10})V^VO_{40}.13H_2O$ (Björnberg & Hedman, 1980). In order to characterize the system further we have applied other methods such as ^{51}V NMR and Raman and IR spectroscopy. The necessity of these complementary methods is easily understood by a comparison between the anion discussed in this paper and the one in $Na_6Mo_6V_2O_{26}.16H_2O$. The anions have different configurations, but the same composition ($Mo_6V_2O_{26}^{6-}$) and cannot therefore be separated by the conventional e.m.f. technique.

Table 1. *Fractional atomic coordinates and B_{eq} values (Hamilton, 1959) with e.s.d.'s in parentheses*

The index in the O designation O(*i*), O(*i,j*), O(*i,j,k*...) denotes to which Mo and/or V each O is coordinated.

	x	y	z	B_{eq}(Å^2)
Mo(1)	0·07018 (2)	0·17345 (2)	0·23090 (4)	0·99 (1)
Mo(2)	0·27076 (4)	0	0·46363 (6)	1·09 (1)
V(3)	0·11554 (6)	0	−0·00720 (10)	0·72 (2)
O(1)	0·0786 (2)	0·3035 (2)	0·1999 (4)	1·59 (13)
O′(1)	0·0425 (2)	0·1641 (2)	0·3898 (4)	1·79 (15)
O(12)	0·2302 (2)	0·1424 (2)	0·3851 (3)	1·23 (11)
O(131)	0·0852 (2)	0·1447 (2)	−0·0042 (3)	0·97 (10)
O(12313)	0·0676 (3)	0	0·1952 (5)	1·02 (12)
O(2)	0·4178 (3)	0	0·5963 (6)	1·88 (16)
O′(2)	0·2420 (4)	0	0·6227 (6)	2·04 (21)
O(23)	0·2519 (3)	0	0·2017 (5)	1·18 (12)
O(3)	0·1355 (3)	0	−0·1639 (5)	1·50 (15)
Na	$\frac{1}{2}$	$\frac{1}{2}$	$\frac{1}{2}$	3·76 (26)
K(1)	0	$\frac{1}{2}$	0	3·84 (14)
K(2)	0·2875 (1)	0·3062 (1)	0·2322 (2)	3·06 (7)
Aq	0·3691 (3)	0·1369 (4)	0·1419 (7)	4·43 (31)

Experimental. In the crystal preparation 7·26 g $Na_2MoO_4.2H_2O$ (0·03 mol), 1·40 g $NaVO_3.H_2O$ (0·01 mol) and 5·22 g KCl (0·07 mol) were each individually dissolved in 50 ml of water (the second in boiling water). The molybdate solution was poured into the vanadate solution and 13·33 ml 3 *M* HCl (0·04 mol) added dropwise while stirring. After addition of the KCl solution and filtration, the solution was set to evaporate at room temperature. Within one or two weeks, yellow prismatic crystals were formed. D_m was measured by pycnometry (*m*-xylene). The crystals seemed to be stable in air, but the one used for the X-ray investigation (of approximate size 0·13 × 0·16 × 0·11 mm) was kept in a glass capillary with part of the mother liquor.

Syntex *R*3 four-circle diffractometer, graphite-monochromatized Mo $K\bar{\alpha}$; cell parameters by least-squares refinement from 25, automatically centered, reflexions ($18° < 2\theta < 27°$); θ–2θ scan, $5° \leq 2\theta \leq 90°$, $0 \leq h \leq 29$, $0 \leq k \leq 25$, $-18 \leq l \leq 14$; 5946 reflexions measured, 5801 unique, 3973 observed [$I \geq 3\sigma(I)$]; 2θ scan rate 2–6° min^{-1}, 2θ scan width 2·8° plus the α_1–α_2 dispersion, background measured on each side of the peak for a total time equal to the scan time; 5 standard reflexions ($3\bar{1}\bar{3}$, $00\bar{4}$, $39\bar{5}$, 262, 244) measured every 50 reflexions, maximum variation $\pm 3·5\%$; empirical absorption correction, 21 reflexions evenly distributed in 2θ, each reflexion being rotated around its diffraction vector in steps of 10°, relative transmission factor 0·692–1·000; Lp correction; Patterson synthesis and standard heavy-atom methods; anisotropic full-matrix least-squares refinements minimizing $\sum w(|F_o| - |F_c|)^2$. Final $R = 0·043$, $wR = 0·052$, $S = 1·932$ for 114 refined parameters, $1/w = \sigma^2(F_o) + (0·015\,F_o)^2$ with $\sigma(F_o)$ from counting statistics. Three of the strong reflexions had F_c 8–15% greater than F_o, but no extinction correction was made because of problems with properly measuring the crystal. These reflexions were instead excluded from the final refinements and are marked with an asterisk in the F_o/F_c list. $(\Delta/\sigma)_{\rm max} = 0{\cdot}01$ [β_{12} for O(131)]. $(\Delta\rho)_{\rm max} = 2{\cdot}68$, $(\Delta\rho)_{\rm min} = -2{\cdot}27$ e Å^{-3}. Scattering factors used were Mo^{3+}, V^{2+}, O$^-$ for anion O, and O for waterO; account was taken of the anomalous dispersion (*International Tables for X-ray Crystallography*, 1974). Attempts to locate the H atoms were not successful. The computer programs used were those supplied with the Syntex $R3$ crystallographic system and those described by Antti (1976). Computations were performed with the Data General Nova 3 computer at this Department and the CDC Cyber 730 computer at the University Computer Centre.

Discussion. The structure comprises discrete Mo$_6$V$_2$O$_{26}^{6-}$ anions, Na$^+$ and K$^+$ cations and water molecules. Final positional parameters, together with $B_{\rm eq}$ values, of the nonhydrogen atoms are given in Table 1.*

The anions, with crystallographic symmetry $2/m$ and the center at (0,0,0), consist of six MoO$_6$ and two VO$_6$ octahedra sharing edges (Fig. 1). As can be seen from Table 2 the octahedra are greatly distorted, but show the same distribution between short, intermediate and long bonds as the octahedra in the β-Mo$_8$O$_{26}^{4-}$ anion. The minimum and maximum values of the corresponding distances in a number of octamolybdates are given within square brackets (Román, Jaud & Galy, 1981; Román, Martínez-Ripoll & Jaud, 1982; Román, Vegas, Martínez-Ripoll & García-Blanco, 1982; Kroenke, Fackler & Mazany, 1983; Bharadwaj, Ohashi, Sasada, Sasaki & Yamase, 1984; McCarron & Harlow, 1984). It is obvious that introduction of the two VO$_6$ octahedra affects the size of the anion. The M—M and M—O distances marked with an asterisk in Table 2 are significantly shorter in the Mo$_6$V$_2$O$_{26}^{6-}$ anion compared with the shortest value for the octamolybdate. The angles have remained unchanged except for O(1)—Mo(1)—O′(1), O(12313)—Mo(1)—O(131)$^{\rm i}$, O(131)—Mo(1)—O(131)$^{\rm i}$ and O(12313)—V(3)—O(12313)$^{\rm i}$ which have become significantly larger (0·3, 1·3, 0·5 and

Table 2. *Selected distances* (Å) *and angles* (°) *within the* Mo$_6$V$_2$O$_{26}^{6-}$ *anion*

The values within square brackets are the minimum and maximum values, from the corresponding M—M and M—O distances, in the β-Mo$_8$O$_{26}^{4-}$ anions referred to in the text.

Mo(1)—Mo(1)$^{\rm i}$	3·337 (1)*	[3·393 (1)–3·457 (1)]
Mo(1)—Mo(2)	3·242 (1)	[3·227 (2)–3·288 (1)]
Mo(1)—V(3)	3·443 (1)*	[3·497 (1)–3·555 (1)]
Mo(1)—V(3)$^{\rm i}$	3·125 (1)*	[3·200 (1)–3·232 (1)]
Mo(2)—V(3)	3·380 (1)*	[3·429 (1)–3·499 (1)]
V(3)—V(3)$^{\rm i}$	3·494 (1)*	[3·536 (1)–3·610 (1)]
Mo(1)—Mo(1)$^{\rm ii}$	4·461 (1)*	[4·551 (1)–4·645 (1)]
Mo(2)—V(3)$^{\rm i}$	4·540 (1)	[4·513 (1)–4·641 (1)]

Mo(1)—O(1)	1·713 (3)	[1·692 (6)–1·716 (3)]
Mo(1)—O′(1)	1·725 (3)	[1·688 (3)–1·718 (7)]
Mo(1)—O(12)	1·906 (2)	[1·879 (3)–1·908 (2)]
Mo(1)—O(131)$^{\rm i}$	1·955 (2)*	[1·981 (3)–2·015 (5)]
Mo(1)—O(131)	2·304 (2)	[2·286 (5)–2·382 (4)]
Mo(1)—O(12313)	2·251 (1)*	[2·271 (2)–2·368 (2)]

O(1)—Mo(1)—O′(1)	106·5 (1)	O(12313)—Mo(1)—O(131)$^{\rm i}$	75·9 (1)
O(1)—Mo(1)—O(12)	98·2 (1)	O(12313)—Mo(1)—O(131)	73·2 (1)
O(1)—Mo(1)—O(131)$^{\rm i}$	99·8 (1)	O′(1)—Mo(1)—O(12)	101·4 (1)
O(1)—Mo(1)—O(131)	87·0 (1)	O′(1)—Mo(1)—O(131)$^{\rm i}$	97·8 (1)
O(12313)—Mo(1)—O′(1)	93·4 (1)	O(131)—Mo(1)—O(12)	82·1 (1)
O(12313)—Mo(1)—O(12)	78·5 (1)	O(131)—Mo(1)—O(131)$^{\rm i}$	73·5 (1)

Mo(2)—O(2)	1·717 (4)	[1·686 (5)–1·711 (2)]
Mo(2)—O′(2)	1·735 (5)	[1·697 (5)–1·724 (5)]
Mo(2)—O(12)	1·921 (2)	[1·909 (6)–1·940 (6)]
Mo(2)—O(23)	2·214 (3)*	[2·273 (4)–2·293 (2)]
Mo(2)—O(12313)	2·437 (3)	[2·420 (2)–2·537 (3)]

O(2)—Mo(2)—O′(2)	105·6 (2)	O(12313)—Mo(2)—O(12)	73·7 (1)
O(2)—Mo(2)—O(12)	103·4 (1)	O(12313)—Mo(2)—O(23)	70·4 (1)
O(2)—Mo(2)—O(23)	91·2 (2)	O′(2)—Mo(2)—O(12)	97·4 (1)
O(12313)—Mo(2)—O′(2)	92·8 (2)	O(23)—Mo(2)—O(12)	78·3 (1)

V(3)—O(3)	1·618 (4)*	[1·683 (3)–1·704 (2)]
V(3)—O(23)	1·717 (3)*	[1·739 (4)–1·767 (4)]
V(3)—O(131)	1·918 (2)*	[1·934 (2)–1·962 (3)]
V(3)—O(12313)$^{\rm i}$	2·132 (3)	[2·128 (4)–2·159 (2)]
V(3)—O(12313)	2·337 (3)	[2·340 (2)–2·409 (3)]

O(3)—V(3)—O(23)	104·1 (2)	O(12313)—V(3)—O(131)	78·6 (1)
O(3)—V(3)—O(131)	100·5 (1)	O(12313)—V(3)—O(12313)$^{\rm i}$	77·3 (1)
O(3)—V(3)—O(12313)$^{\rm i}$	97·2 (2)	O(23)—V(3)—O(131)	96·3 (1)
O(12313)—V(3)—O(23)	81·4 (1)	O(12313)$^{\rm i}$—V(3)—O(131)	79·6 (1)

Symmetry code: (i) $\bar{x}, y, \bar{z}$; (ii) $x, \bar{y}, z$.

* Distance statistically shorter than the values within square brackets.

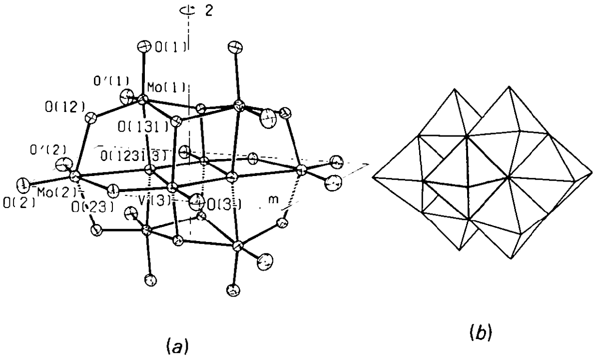

Fig. 1. (*a*) A perspective view of the Mo$_6$V$_2$O$_{26}^{6-}$ anion. Only the unique atoms are labeled. The thermal ellipsoids are, here and elsewhere, scaled to include 50% probability (*ORTEP*II; Johnson, 1976). (*b*) The same anion, turned 15° clockwise round the twofold axis, and drawn as linked polyhedra. The VO$_6$ polyhedra are, as in Fig. 2(*a*), shaded.

---

* Lists of structure factors, anisotropic thermal parameters and O—O distances within the anion have been deposited with the British Library Lending Division as Supplementary Publication No. SUP 42439 (19 pp.). Copies may be obtained through The Executive Secretary, International Union of Crystallography, 5 Abbey Square, Chester CH1 2HU, England.

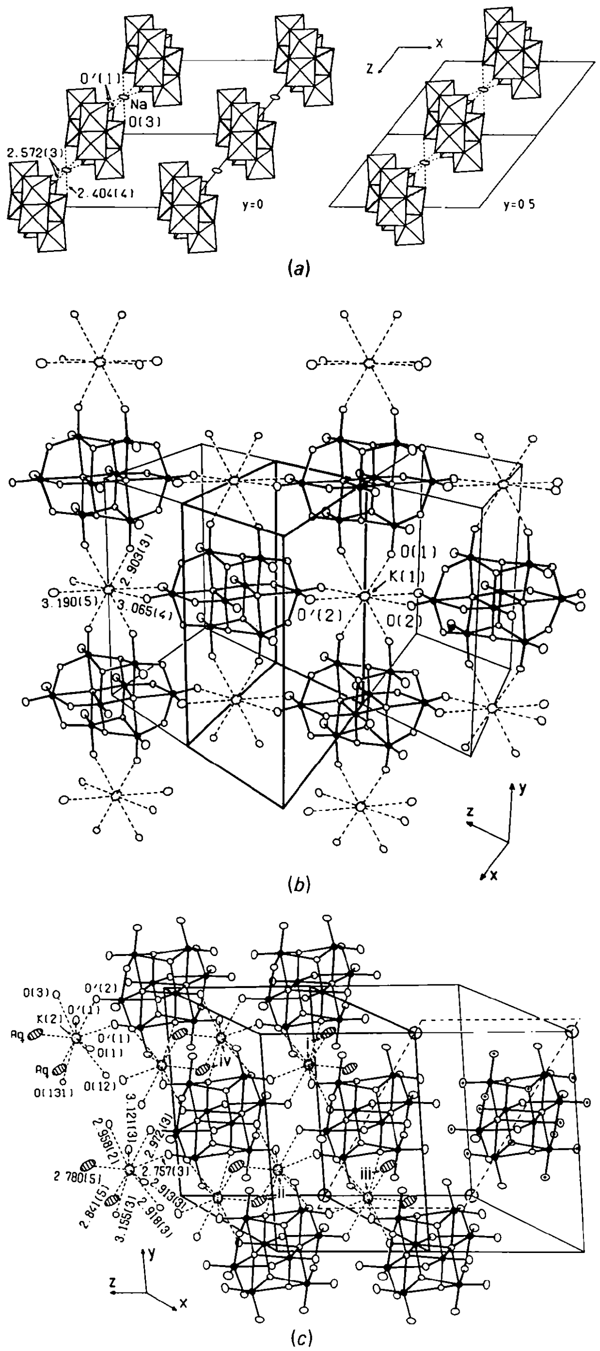

Fig. 2. The anion–cation and cation–water arrangement with bond lengths (Å). (*a*) The O–Na–O bridges viewed approximately down the y axis. The anions are drawn as linked polyhedra. (*b*) The O–K(1)–O bridges. Only one layer is shown. (*c*) The O–K(2)–O bridges. On the left part of the diagram, one layer parallel to (110) is shown. Symmetry operations: (i) $x, 1-y, z$; (ii) $1-x, y, 1-z$; (iii) $\frac{1}{2}+x, \frac{1}{2}-y, z$; (iv) $\frac{1}{2}-x, \frac{1}{2}+y, 1-z$. The remaining cations and water molecules, related to (i)–(iv) by a mirror plane at $y = 0.5$, in the same way take part in bondings in the layer parallel to $(\bar{1}10)$. A schematic representation of this layer is shown to the right. The anions at (0,0,0) are drawn as circles and in one of the anions at ($\frac{1}{2},\frac{1}{2}$,0) the O's included in the K(2)–O interactions are marked with dots.

0·5°, respectively) and O(1)–Mo(1)–O(12) which has become smaller (0·5°) compared with the corresponding nearest value in β-$Mo_8O_{26}^{4-}$. The V(3)–O(3) distance is in good agreement with the V–O(terminal) distances in the $V_{10}O_{28}^{6-}$ anion, *e.g.* in $Ca_3V_{10}O_{28}.17H_2O$ (Swallow, Ahmed & Barnes, 1966) and $Er_2V_{10}O_{28}.25H_2O$ (Rivero, Rigotti, Punte & Navaza, 1984), where it varies between 1·59–1·62 Å. The reduced size of the anion probably depends on the smaller electrostatic repulsion between V^V–V^V and Mo^{VI}–V^V than between two Mo^{VI}. Furthermore, since V^V occupies the two central octahedra in the anion and their size is somewhat smaller than for Mo^{VI}, the shortening of the Mo(1)–Mo(1)^{i} and Mo(1)–Mo(1)^{ii} distances may easily be understood.

The coupling between the anions through Na^+ and K^+ cations can be separated into three groups: (i) O–Na–O bridges forming chains parallel to the z axis (Fig. 2*a*), (ii) O–K(1)–O bridges forming layers parallel to $(20\bar{1})$ (Fig. 2*b*) and (iii) O–K(2)–O bridges forming two intersecting layers parallel to (110) and $(\bar{1}10)$, respectively (Fig. 2*c*). Together, these three groups form a very stable arrangement where every anion is linked to two Na, four K(1) and 12 K(2) cations. It is noteworthy that among the 26 anion O there are only four which are not included in any Na/K–O interaction, namely: O(23), O(23)^{i} and the more or less inaccessible O(12313) and O(12313)^{i} [(i) $\bar{x},y,\bar{z}$]. Furthermore, the Aq–O distances indicate that the water molecule takes part in hydrogen bonds: Aq–O(23) 2·746 (5), Aq–O(1)^{i} 2·904 (5) and Aq–O(2)^{ii} 3·073 (5) Å [(i) $\frac{1}{2}+x, \frac{1}{2}-y, z$; (ii) $1-x, y, 1-z$].

To distinguish this new isomer of the $Mo_6V_2O_{26}^{6-}$ anion from the one determined by Björnberg (1979*b*) a comparison with the two configurations of the octamolybdate could be made and the same notation used. The anion in $Na_6Mo_6V_2O_{26}.16H_2O$ consists of six MoO_6 octahedra joined together by common edges to form a flat ring which is capped on each side by a VO_4 tetrahedron. The anion has the same configuration as α-$Mo_8O_{26}^{4-}$ (Fuchs & Hartl, 1976) and may therefore be named α-$Mo_6V_2O_{26}^{6-}$. In the same way the anion described in this paper may, in comparison with β-$Mo_8O_{26}^{4-}$, be designated β-$Mo_6V_2O_{26}^{6-}$.

I wish to thank Professor Nils Ingri for his great interest and for all the facilities placed at my disposal, and Drs Britt Hedman and Lage Pettersson for valuable comments on the manuscript. This work is part of a program financially supported by the Swedish Natural Science Research Council.

References

Antti, B.-M. (1976). *Acta Chem. Scand. Ser. A*, **30**, 24–30.
Bharadwaj, P. K., Ohashi, Y., Sasada, Y., Sasaki, Y. & Yamase, T. (1984). *Acta Cryst.* C**40**, 48–50.

BJÖRNBERG, A. (1979*a*). *Acta Cryst.* B**35**, 1989–1995.
BJÖRNBERG, A. (1979*b*). *Acta Cryst.* B**35**, 1995–1999.
BJÖRNBERG, A. (1980). *Acta Cryst.* B**36**, 1530–1536.
BJÖRNBERG, A. & HEDMAN, B. (1980). *Acta Cryst.* B**36**, 1018–1022.
FUCHS, J. & HARTL, H. (1976). *Angew. Chem.* **88**, 385–386.
HAMILTON, W. C. (1959). *Acta Cryst.* **12**, 609–610.
International Tables for X-ray Crystallography (1974). Vol. IV, pp. 72–98, 149–150. Birmingham: Kynoch Press. (Present distributor D. Reidel, Dordrecht.)
JOHNSON, C. K. (1976). *ORTEP*II. Report ORNL-5138. Oak Ridge National Laboratory, Tennessee.
KROENKE, W. J., FACKLER, J. P. JR & MAZANY, A. M. (1983). *Inorg. Chem.* **22**, 2412–2416.
LINDQVIST, I. (1950). *Ark. Kemi*, **2**, 349–355.
MCCARRON, E. M. III & HARLOW, R. L. (1984). *Acta Cryst.* C**40**, 1140–1141.
MELLOR, J. W. (1964). *A Comprehensive Treatise on Inorganic and Theoretical Chemistry*, Vol. IX, pp. 780–784. London: Longmans.
PETTERSSON, L. (1984). Private communication.
RIVERO, B. E., RIGOTTI, G., PUNTE, G. & NAVAZA, A. (1984). *Acta Cryst.* C**40**, 715–718.
ROMÁN, P., JAUD, J. & GALY, J. (1981). *Z. Kristallogr.* **154**, 59–68.
ROMÁN, P., MARTÍNEZ-RIPOLL, M. & JAUD, J. (1982). *Z. Kristallogr.* **158**, 141–147.
ROMÁN, P., VEGAS, A., MARTÍNEZ-RIPOLL, M. & GARCÍA-BLANCO, S. (1982). *Z. Kristallogr.* **159**, 291–295.
SWALLOW, A. G., AHMED, F. R. & BARNES, W. H. (1966). *Acta Cryst.* **21**, 397–405.

Acta Cryst. (1985). C**41**, 1707–1709

Dilithium Magnesium Zirconium Tetraoxide with an α-$LiFeO_2$ Structure

BY M. CASTELLANOS

División Estudios de Posgrado, Facultad de Química, UNAM, México, DF 04510 *Mexico*

AND A. R. WEST AND W. B. REID

*University of Aberdeen, Department of Chemistry, Meston Walk, Aberdeen AB*9 2*UE, Scotland*

(*Received* 29 *October* 1984; *accepted* 8 *July* 1985)

Abstract. Li_2MgZrO_4. Formed by solid-state reaction of Li_2ZrO_3 and MgO; isostructural with α-$LiFeO_2$ [Posnjak & Barth (1931). *Phys. Rev.* **38**, 2234–2239] but with Mg, Zr disordered over Fe sites. $M_r = 193{\cdot}41$, tetragonal, $I4_1/amd$, $a = 4{\cdot}209$ (1), $c = 9{\cdot}145$ (2) Å, $V = 162{\cdot}010$ Å^3, $Z = 2$, $D_x = 3{\cdot}964$ g cm^{-3}, Cu $K\alpha_1$, $\lambda = 1{\cdot}5405$ Å, $\mu = 27{\cdot}1$ mm^{-1}, $F(000) = 180$, powdered sample, room temperature, $R = 0{\cdot}033$ for 16 unique reflections. Li—O bond lengths are 2·110 (1) and 2·441 (15) Å, the latter being abnormally long, and Mg, Zr—O are 2·110 (1) and 2·132 (15) Å.

Introduction. In the family of oxides that have rock-salt and ordered rock-salt structures, various cation-ordering sequences are possible with phases containing >1 cation. We are interested in the synthesis of new ordered and partially ordered structures, their solid solutions and phase transitions and describe here the synthesis and structure of one such phase, Li_2MgZrO_4.

Experimental. Li_2MgZrO_4 prepared by solid-state reaction of Li_2ZrO_3 and MgO. Li_2ZrO_3 first prepared by reaction of equimolar amounts of Li_2CO_3 and ZrO_2 (Analar grade) in a Pt crucible in a muffle furnace. Reaction mixture heated initially at 870 to 970 K for a few hours to expel CO_2 followed by 1 to 2 d at 1170 K. For the reaction of Li_2ZrO_3 and MgO to produce Li_2MgZrO_4, higher temperatures were found to be necessary, ~1370 K; at these temperatures loss of lithia by volatilization was a serious problem that could not be overcome simply by placing a lid on the crucible. The method that was adopted, successfully, to avoid lithia loss was to carry out reaction in pelleted samples and to have pellets immersed completely in pre-sintered powder of the same composition. The pellets, with covering powder, were fired in covered Pt crucibles at 1320 K for 24 h.

Reaction product(s) analysed by X-ray powder diffraction, Philips Hägg Guinier camera, Cu $K\alpha_1$ radiation, KCl as internal standard for accurate *d*-spacing measurements, Philips PW 1050/25 diffractometer for intensity measurements, flat sample, Cu $K\alpha$ radiation, scan speed $\frac{1}{8}°$ 2θ min^{-1}. Powder pattern of Li_2MgZrO_4 fairly simple with relatively few peaks; a search through the X-ray powder diffraction file, treating it as an unknown, showed its pattern to be very similar to those of phases such as $LiScO_2$ and α-$LiFeO_2$. These have ordered rock-salt structures with a tetragonal unit cell. X-ray powder pattern of Li_2MgZrO_4 was indexed by analogy with that of α-$LiFeO_2$ and accurate unit-cell dimensions obtained by least-squares refinement using 16 unique reflections.

As a starting hypothesis for the structure of Li_2MgZrO_4, it was assumed to be derived from the

0108-2701/85/121707-03$01.50